Region - Water Conservancy, 2026, Volume9, Issue1
DOI: 10.32629/rwc.v9i1.5286
ISSN Online: 2630-4902

Hydrogeology and aquifer conceptual model of Petorca's upper basin (Valparaíso, Chile)

Justinne Andrea Rybertt Goldammer
Universidad Andrés Bello (UNAB), Chile. jrybertt.g@gmail.com

Abstract: For over a decade, Chile has been experiencing an intense drought, with the central region, including the town of Petorca, being one of the most severely affected. Therefore, the purpose of this study is to contribute information to improve water management in the Petorca basin by detailing the functioning of the upper Petorca aquifer, the predominant recharge type, groundwater circulation, and the factors affecting its composition and availability. To achieve this, data collection and field campaigns were conducted. The resulting data were used to create piezometric maps, characterize the groundwater hydrochemistry, perform a water balance analysis for the years 2010-2018, and finally, develop a conceptual model of the Petorca aquifer.

The results of these analyses show that it is an unconfined aquifer whose geometric configuration is controlled by regional structures trending NS to NW. Furthermore, the study explores how the influence of both natural and anthropogenic factors has led to a decrease in both the quality and availability of groundwater over time, with human activity having the greatest impact on the water's characteristics.

Key words: hydrogeology; Petorca aquifer; underground water; water balance, conceptual model

1 Introduction

The importance of groundwater in nature is reflected in its contribution to the hydrological cycle; in addition, it is a renewable natural resource and of essential importance to civilization. It is used for the supply of drinking water in both individual homes and urban areas, in agricultural projects, and in many industries that consume large quantities of water, such as mining (Vélez, 1999).

The chemical composition of groundwater is the result of continuous interaction processes between rainwater that infiltrates the ground and the rocks through which it flows (González-Abraham, 2012). The role of human activity in its chemical composition should be emphasized, as it causes a progressive deterioration in the quality of both surface and groundwater (Fagundo, 2010).

In the Petorca commune, as in many parts of the country, there is a severe water shortage, which has resulted in the Petorca River being mostly dry. The main uses of water in this area are fruit farming, followed by the mining industry and the supply of drinking water (INE, 2007). However, extraction is so extensive that it has left some areas without water for this last use (Department of Water Resources, 2016).

While the problems affecting the Petorca Valley are known, only fragmented data on the characteristics and/or properties of the aquifer in the upper part of the basin are available. Therefore, there is no clarity regarding how it functions, the materials that compose it and its dimensions, as well as the movement of groundwater and the factors that control it.

According to Cica et al. (1979), in the Petorca River basin, a poor aquifer and possible confined aquifers are found in the older sediments, while a more unconfined aquifer with better characteristics is located in the layer of recent sediments within the first 5 to 30 m. Cade-Idepe Consultores (2004) agrees with Cica, noting that the thickness of the recent deposits, where the upper aquifer is located, varies between 8 and 25 m. On the other hand, the National Hydrogeological Map suggests that the thickness of the upper aquifer would not exceed 10 m. Furthermore, GCF Ingenieros Ltda. (2011) states that there is no clear differentiation of aquifers, indicating that predominantly unconfined aquifers are observed, with only local stratigraphic variations.

Defining the hydrogeological conceptual model, conducting a water balance, and analyzing the composition of the waters in the area will help answer these questions. This information will be made available to the community and authorities to advance toward sustainable water use management.

Many of the results in this article are based on the work of Rybertt (2019).

2 Study area

The study area (Figure 1) is located on the northeastern border of the Valparaíso Region, comprising the first three sub-basins of Petorca, namely the Pedernales River, the Sobrante River, and the Petorca Oriente River, covering 1,018 km². Within these is the Petorca aquifer, limited to fluvio-alluvial deposits with an area of 80.6 km².

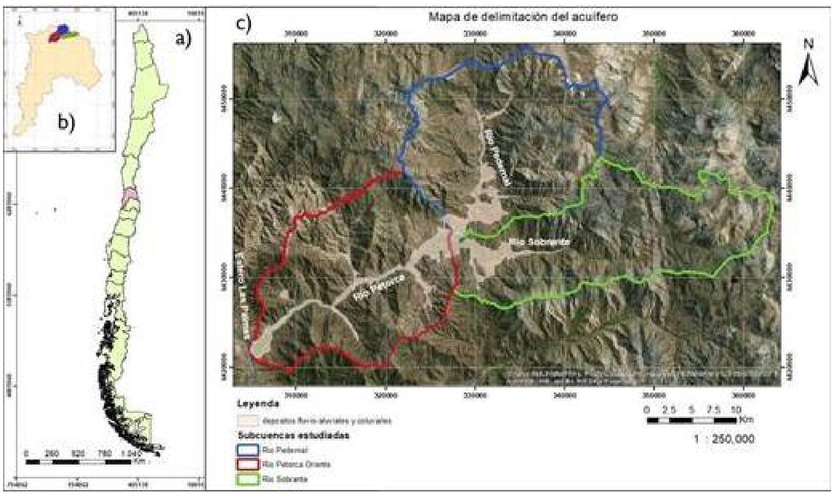

Figure 1. Location of the study area

Geologically (Figure 2), it is characterized by stratified sedimentary, volcanic, and volcaniclastic rocks of continental origin and intrusive units, arranged in NS-trending bands with ages ranging from the Lower Cretaceous to the Upper Tertiary (Rivano, 1993). The basement of this basin is considered practically impermeable, except in particular cases where, due to fracturing associated with extensional-compressive tectonic processes or other variables that increase the degree of permeability of the system, structural slopes are formed (GCF Ingenieros Ltda., 2011).

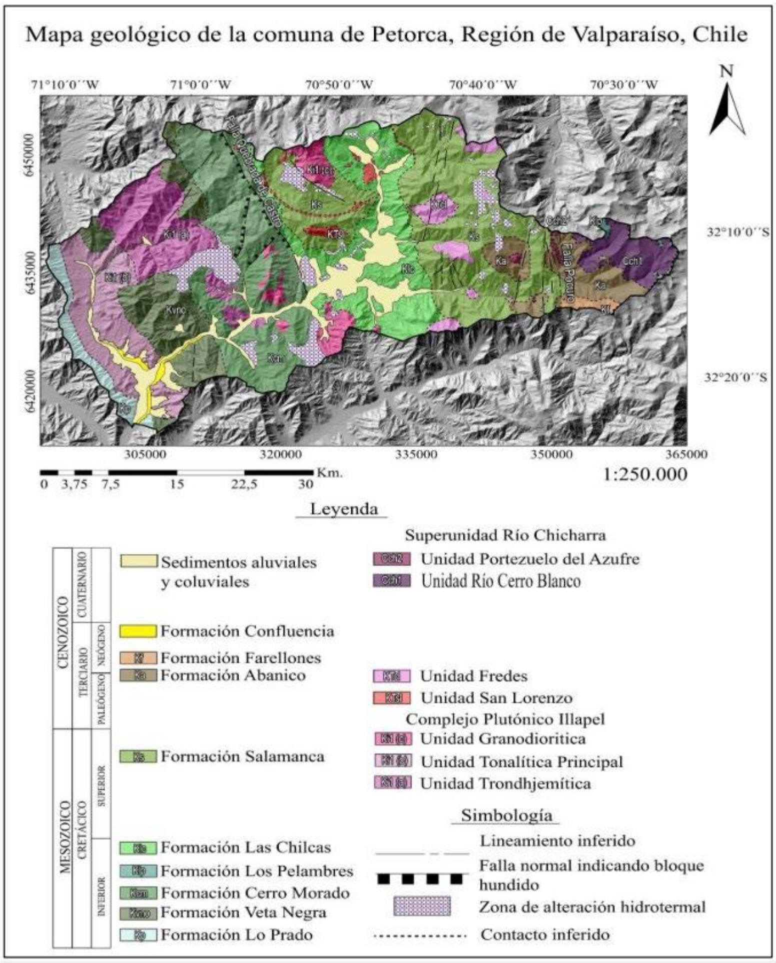

Figure 2. Geological map of the Petorca commune (Pérez, 2018)

Compilation based on (Rivano et al., 1993), (Camus et al., 1991), (Jara, 2013) and (Ferrando, 2014)

3 Materials and methods

The methodologies in this study are divided by area of work (Figure 3).

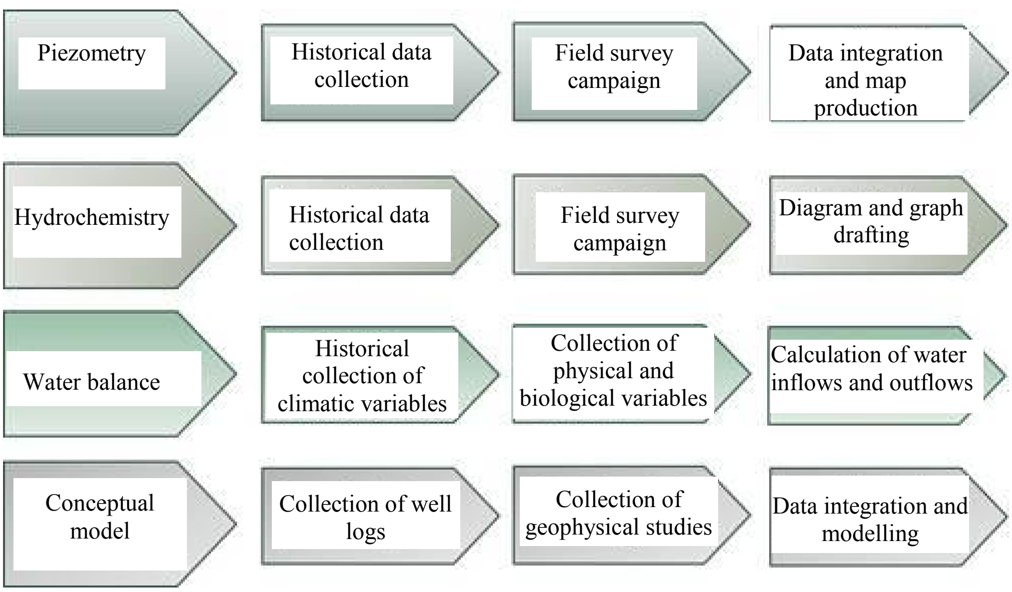

Figure 3. Methodological phases by area of study

3.1 Piezometry

Initially, information was collected from 1995 to 2019 on daily static levels measured at stations belonging to the General Directorate of Water (Annex 1). This data was compared with the precipitation that occurred in the same period (Figures 7 and 8), obtained from the CAMELS-CL database (Alvarez-Garreton, 2018).

During the field campaign, wells belonging to Rural Potable Water (APR) committees and private wells were measured. The location and altitude of each well were recorded using a Garmin eTrex 10X GPS (GCS WGS84), and the depth to the water table was measured using a 50 m Solinist well gauge (Figure 4). Piezometric maps (Figures 5 and 6) were created from this data using the Inverse Distance Weighting (IDW) tool in ArcGIS Desktop 10.8.1. The piezometric levels were interpolated and corrected according to the researchers' interpretation.

Figure 4. Materials used in field campaigns

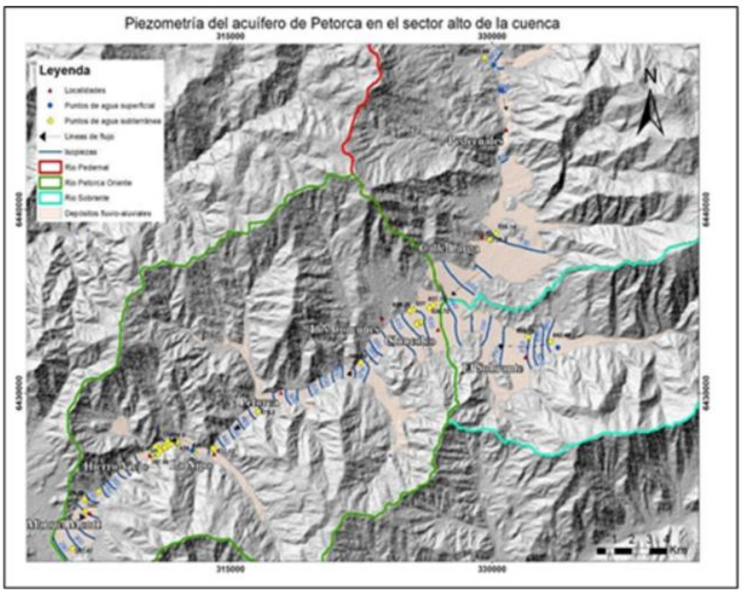

Figure 5. Piezometric map of the upper sector of the Petorca Aquifer based on a DEM satellite image

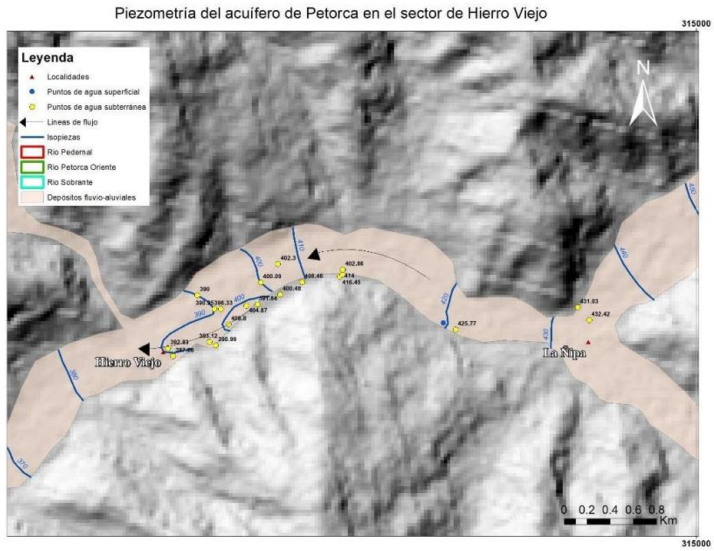

Figure 6. Piezometric map of the Hierro Viejo sector based on a DEM satellite image

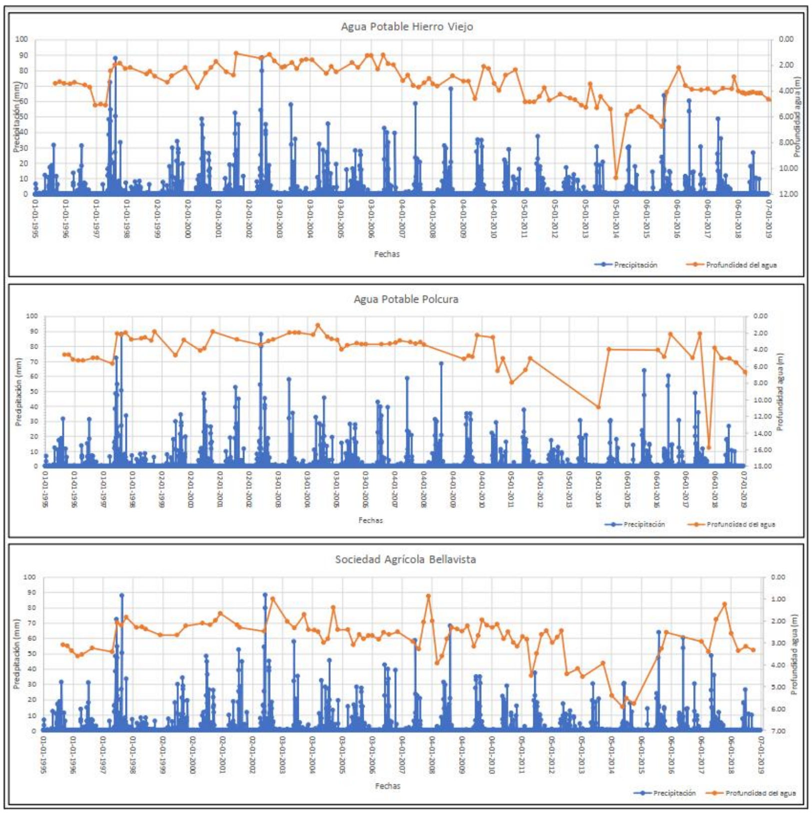

Figure 7. Chronological comparison between precipitation (blue) and static water levels (orange) for the stations within the Río Petorca Oriente sub-basin.

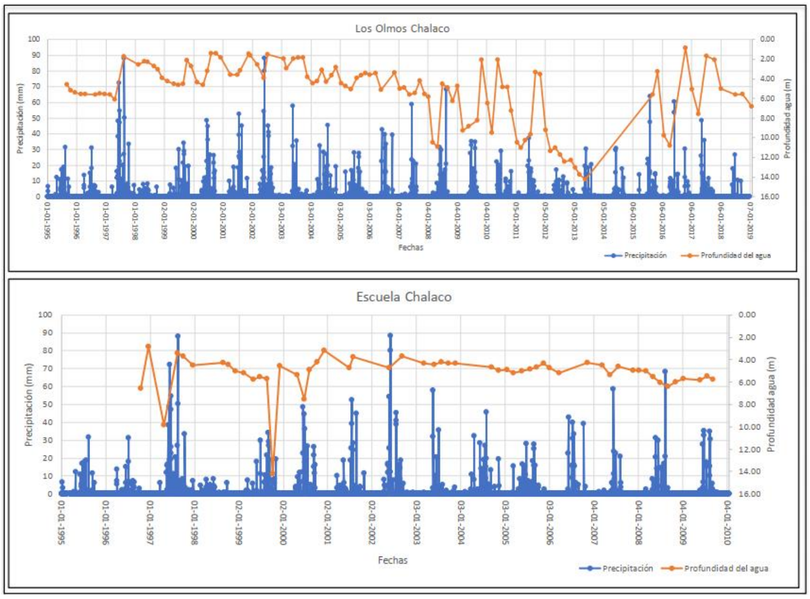

Figure 8. Chronological comparison between precipitation (blue) and static levels (orange) of the stations included in the Río Pedernal sub-basin.

3.2 Hydrochemistry

To study the hydrochemical evolution of the water, data were collected through the online statistics system of the General Directorate of Water (DGA) at three physicochemical parameter monitoring stations (Appendix 1). The data on major ions covers the period from 1984 to 2006, at which point bicarbonate measurements ceased at all stations. However, groundwater quality monitoring reports from wells in the Valle los Olmos Rural Potable Water System (APR) for the years 2015, 2016, and 2017 were used to analyze the most current water conditions. The data were processed using the free software Diagrammes 5.4 (SIMLER, 2018), where the analytical error and Pearson correlation matrix were calculated (Appendix 2). Piper (Figure 9), Stiff (Figure 11), and binary (Figure 10) diagrams were also generated to classify the types of water present.

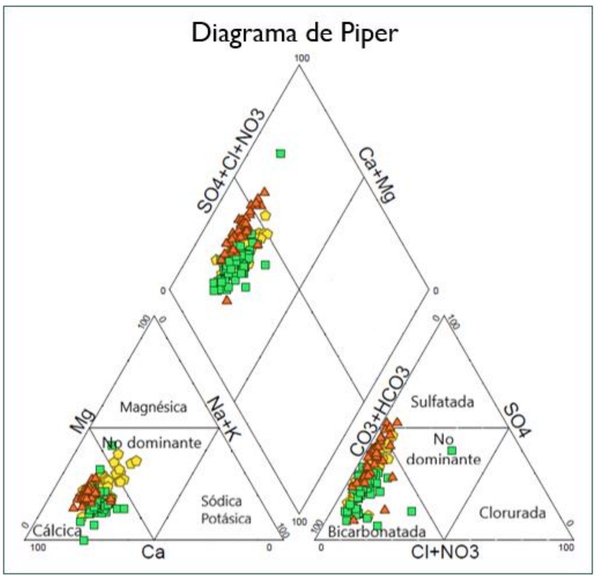

Figure 9. Piper diagram with data obtained from the DGA

Orange triangles represent the Pedernal River in Tejada, green squares represent the Sobrante River in Piñadero, and yellow pentagons represent the Petorca River in Petorca.

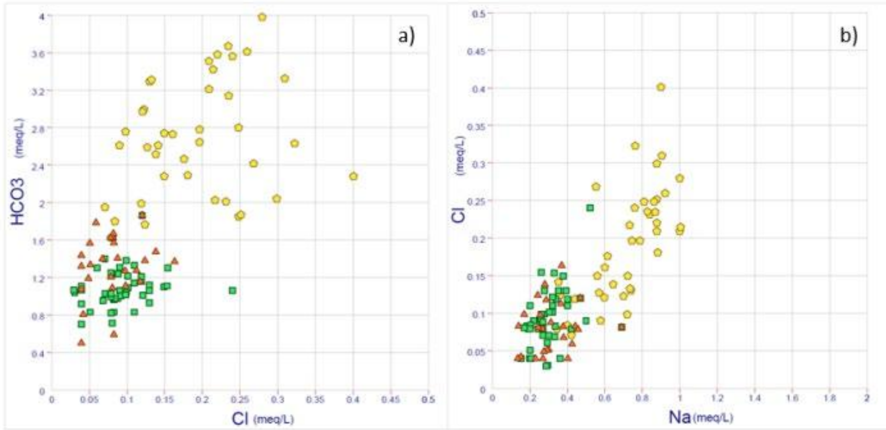

Figure 10. Binary graphs of concentrations in a) Cl/HCO3 and b) Na/Cl

In orange triangles, the Pedernal River in Tejada is represented, in green squares, the Sobrante River in Piñadero, and in yellow pentagons, the Petorca River in Petorca.

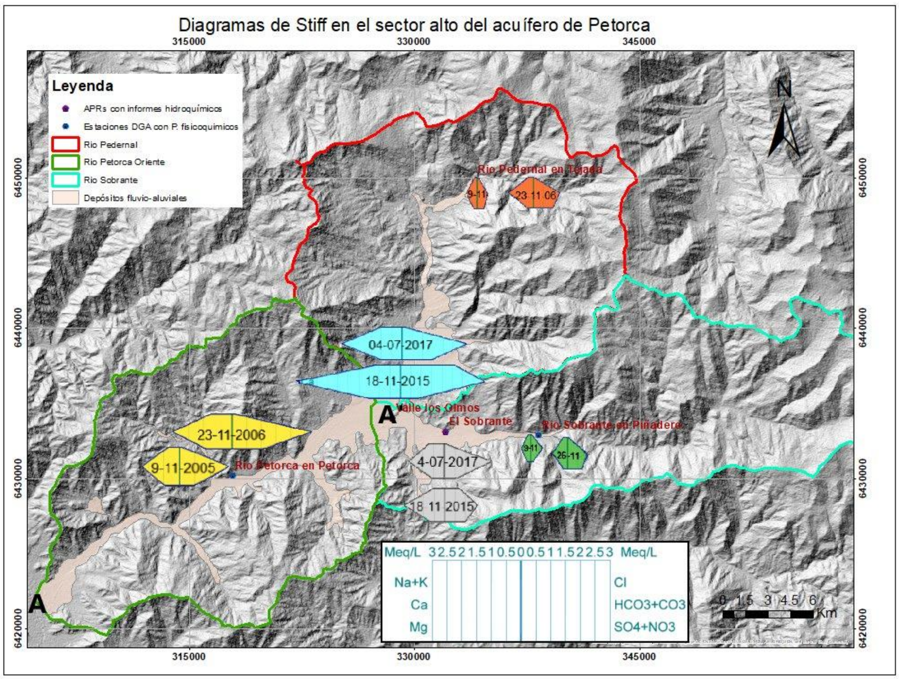

Figure 11. Stiff diagram distributions in the upper sector of the Petorca aquifer

During the field campaign, water samples are taken from the wells using a bailer or the installed extraction pump. These samples are analyzed with a Hanna HI 9828 multiparameter meter (Figure 4), measuring pH, electrical conductivity (EC), total dissolved solids (TSD), temperature, oxidation-reduction potential (ORP), and dissolved oxygen (DO).

3.3 Meteorological balance 2010-2018

Available information on the aquifer units present in the sector is compiled from previous studies and well records provided by the DGA, obtaining hydraulic parameters such as permeability and transmissivity.

For meteorological data collection, precipitation data was obtained from the DGA network of stations via the web, from which daily precipitation data for the specified years were extracted and the average calculated. For temperature, data from 2010 to 2016 were combined using CAMELS-CL data, and for 2017 and 2018, data from the Chincolco Liceo Agrícola station, belonging to the Chilean Meteorological Directorate, and the Salamanca station, located outside the study area and chosen because it shares the same bioclimatic characteristics as the Petorca Valley (Luebert, 2012), were used. Wind speed, hours of sunshine, radiation, and relative humidity data were also obtained from these stations (Appendix 1), and these were used to calculate evapotranspiration (ETP).

Regarding agricultural information, to calculate the average root thickness of the crops present in the sector, avocados, walnuts and citrus fruits are considered as the main crops (Richard, 1998), to calculate the irrigation supply required in the total crops, the proportion of these is valued according to CIREN (2017).

The area of planted crops varies considerably during the years covered by the hydrometeorological balance. Therefore, to verify the number of hectares planted per year, a crop classification is performed using satellite image analysis in the ENVI 5.6.1 program. First, images were downloaded from the USGS platform, then atmospheric correction and radiometric calibration were applied using the mathematical banding module. Following this, different band combinations were run to distinguish agricultural plantations from natural vegetation in order to carry out a supervised classification to account for the area of agricultural crops present for each year. Since the system does not distinguish between tree types, the crop proportions obtained from the 2017 CIREN survey are used, where avocados represent 64.56%, citrus fruits 22.64%, and walnut trees 11.30%, totaling 98.5% of the total cultivated area. Finally, this information is cross-referenced with the monthly water requirements of avocado trees (Ovalle J. M, 2012), citrus trees (Castillo, 2008) and walnut trees (Lobos G, 2017).

Based on the hydrometeorological balance, the water flow from precipitation and irrigation return that effectively recharges the system annually is estimated. The free software EASYBAL (Vazquez & Serrano, 2013) was used for this calculation, recording the aforementioned daily data. Additionally, field capacity, wilting point, and lamination values, estimated according to soil type using textural classification (Schroeder 1994), must be entered. The software provides annual effective recharge values in [mm/year] without considering the study area. To include the study area, the recharge must be multiplied by the number of hectares, using the surface area of the three sub-basins (101,857 ha), assuming that precipitation throughout the orographic basin would run off into the valley deposits.

3.4 Water balance 2010–2018

For the purposes of the water balance, the valley slopes are assumed to be impermeable, thereby ruling out lateral water inflows. Furthermore, given that the river is largely dry, any river-aquifer interaction is disregarded. Additionally, to compare inflow and outflow rates within the study area, data from DGA gauging stations are used. The parameters considered for this water balance are:

Inflows: Recharge derived from the hydrometeorological balance; losses from water supply and sewerage systems.

Outflows: Extractions (pumping); groundwater outflow across the southwestern boundary of the study area.

To calculate losses associated with water supply and sewerage, the population of the study area is determined (Census, 2017); based on the Superintendence of Sanitary Services (2008) figure of 150 L/day per person, the annual water requirement for the sector's inhabitants is calculated. Finally, the total loss is calculated by applying established rates of 15% for water supply and 5% for sewerage (Girardi & Recio, 2015).

Extraction figures were derived from water rights granted within the study area, as recorded by the General Directorate of Water (Dirección General de Aguas). The extraction value for the years covered by the water balance is calculated by summing the average annual flow rates for each rights holder, expressed in hm^3/year.

Calculating groundwater outflow across the southwestern boundary involves using the flow rate formula for a cross-section (Custodio & Llamas, 1996):

$Q = K * i * b * L$ (1)

Where: K is the hydraulic conductivity and i is the hydraulic gradient.

b, the saturated thickness

L, the transverse length formed by the fluvio-alluvial deposits.

In this study, the K and b values are derived from the literature, whereas i is calculated using field data and L was measured remotely using ArcGIS.

3.5 Conceptual model

Based on the compilation and integration of geophysical (gravimetric profiles), stratigraphic (well logs), structural, and hydrogeological data, a conceptual model is generated; this model incorporates the various variables in an effort to approximate the actual geometry and dynamics of the Petorca aquifer within the study area.

4 Results and discussion

4.1 Piezometry

Groundwater flow is parallel to the river (Figure 5) because the adjacent hillslopes were considered impermeable.

Surface waters are found primarily in the upper reaches of the aquifer along the Pedernal and Sobrante rivers; this may be due to the fact that the fluvio-alluvial deposits in these areas are much thinner than average, and also because there are fewer water withdrawals, given the lower population density and absence of large plantations. The stretch between La Ñipa and Hierro Viejo is the only location downstream where surface water was detected, suggesting that the river exhibits effluent behavior in this sector.

In the Hierro Viejo area, greater detail regarding piezometry was obtained; Figure 6 reveals an increase in the hydraulic gradient, as well as a subsurface flow component along the southern edge of the fluvio-alluvial deposits. This could be attributed to internal structural features of the hill—such as rock fracturing—that create water reservoirs. Studying these systems could prove highly beneficial in the future, following the example of Taucare et al. (2021) in central Chile and recent work led by Linda Daniele.

Comparing annual rainfall with static well levels in the Petorca Oriente sector (Figure 7) reveals a correlation between well levels and rainfall, with levels increasing considerably in rainy years and decreasing when rainfall is low. However, some variations are difficult to attribute to rainfall and could be related to large-scale pumping near the monitoring well, as may have been the case at the Polcura Drinking Water Station in 2017.

In the Pedernal sector (Figure 8)—specifically at Los Olmos Chalaco—a seasonal cyclical pattern is clearly observable: piezometric levels drop during dry periods, while groundwater levels rise during periods of rainfall and accumulated snowmelt. Similar to the situation at A.P. Polcura in 2017, a drop in the static water level was observed at Escuela Chalaco in October 1999 that cannot be attributed to a decrease in precipitation.

In the case of Sobrante, a reliable analysis is not possible due to the limited amount of data.

Regarding storage variation, an examination of just the last five years of monitoring well data shows a rise in the piezometric level—indicating a positive variation; however, this is a relative increase, as the variation is negative when considering the period from 1995 to the present—meaning the volume of stored water has decreased.

4.2 Hydrochemistry

Temperatures range from 16.86 to 21.54°C, with the shallowest wells yielding the warmest water. pH values range from 7.02 to 7.72, showing a fairly homogeneous distribution across the study area. The oxidation-reduction potential (ORP) averages 203.74 mV; the Hierro Viejo sector exhibits the lowest values (187 mV), while values in the Pedernal Valley reach 293 mV. Since all measurements are positive, this may indicate an oxidizing environment. Electrical conductivity (EC) ranges from a minimum of 239 µS/cm in the Pedegua sector to a maximum of 770 µS/cm in Hierro

Viejo. EC values increase significantly downstream of the confluence of the Pedernal and Sobrante rivers; this may be due to the extensive agricultural plantations—where the use of fertilizers and pesticides serves as a major source of mineral salts—or to ongoing mining activity in the area, which could contribute other types of elements.

Total Dissolved Solids (TDS) values range from 132 to 496 ppm, with the Sobrante sector showing the lowest values and Calle Larga the highest. Finally, dissolved oxygen (DO) levels range from 1.03 to 6.91 ppm, decreasing as one moves through the aquifer; oxygen is readily consumed in the presence of oxidizable substances such as organic matter, Fe^{2+}, NH_4^+, and NO^-_2. Consequently, it is inferred that the decrease in this parameter may be attributed to higher urban concentrations and agricultural plantations, which contribute oxidizing substances that consume oxygen through various reactions.

Furthermore, based on the major ions, a Piper diagram (Figure 9) was constructed, identifying primarily calcium-bicarbonate waters in the Sobrante River, calcium-bicarbonate-sulfate waters in the Pedernal River, and calcium-magnesium-bicarbonate waters in the Petorca River. These classifications are consistent with the local geology, which consists mainly of volcano-sedimentary rocks and intermediate-composition granitic intrusive bodies; additionally, bicarbonate waters are characteristic of zones recharged by precipitation.

Based on the rCl^-/HCO_3^- ratio (Figure 10a), the plot indicates the presence of relatively unevolved waters; the youngest waters are located in the Sobrante and Pedernales sectors, whereas those from the Petorca River exhibit higher values, indicating more evolved waters—a finding consistent with the local geography, given that the first two are tributaries of the Petorca River. Furthermore, results from the rNa^+/Cl^- ratio (Figure 10b) and the Pearson correlation matrix (Annex 2) suggest that the dominant hydrogeochemical processes in the study area result from silicate and feldspar weathering. This aligns with the local geology, as the aquifer materials are derived from adjacent rocks—predominantly volcaniclastic rocks and intermediate-composition intrusives—which contain significant proportions of the aforementioned minerals.

The low correlation of the NO_3^- ion with the vast majority of elements analyzed in the Pearson matrix suggests that the source of this substance is not the geological environment; rather, it may be related to the use of nitrogen-containing fertilizers and the decomposition of organic matter from domestic wastewater—whether from septic tanks or leaks in the sewerage system and/or treatment plants (Custodio & Llamas, 1996, v2).

Analysis of the Stiff diagrams for the three aquifer sectors (Figure 11) shows that the Pedernal and Sobrante tributaries have lower major ion concentrations compared to the Petorca station, where calcium and bicarbonate levels are notably high. While this may be attributed to longer water residence times in contact with the lithologies of the fluvio-alluvial deposits, the high concentrations suggest a possible anthropogenic influence—specifically agricultural activity contributing salts via pesticides and fertilizers, and the decomposition of organic matter from both landfill and domestic wastewater (FCIHS, 2009).

4.3 Conceptual model

The conceptual model of the aquifer system's functioning (Figure 12) considers the following factors:

- Inflows: infiltration from precipitation and irrigation return flow, and recharge from losses in water supply and sewer networks. Although runoff from a hillside was observed in the Hierro Viejo sector, it will not be considered because it could not be quantified.
- Outflows: withdrawals via pumping and outflow across the western boundary of the study area.

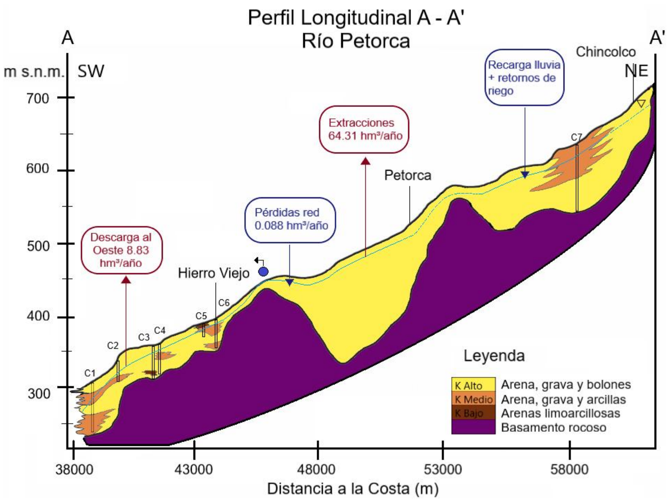

Figure 12. Conceptual model of the hydrogeological functioning of the Petorca fluvial-alluvial aquifer between Chincolco and Manuel Montt. Period considered: January 2010 – December 2018.

The conceptual model was developed extending to the town of Chincolco, as data for the Pedernal and Sobrante sectors are insufficient.

Regarding the hydrogeological units, three main compositional types were distinguished: the most abundant—characterized by highly variable grain sizes—consists of sands, gravels, and cobbles, with a hydraulic conductivity ranging from 1 to 100 m/d and an average effective porosity of 25%. The second unit comprises sands, gravels, and clays with a hydraulic conductivity between 0.01 and 1 m/d; due primarily to their clay content, these deposits are classified as aquifers. The final unit consists of silty-clayey sand lenses with hydraulic conductivities ranging from 10^{-2} to 10^{-4} m/d; these are classified as aquitards—zones of very low permeability that act as hydraulic barriers.

The aquifer's geometry exhibits significant variability in the thickness of the fluvio-alluvial deposits; the maximum thickness of 135 meters is reached between the La Ñipa and Petorca sectors, while the minimum—approximately 1 meter (where water outcrops)—occurs between the Hierro Viejo and La Ñipa sectors. Furthermore, the thickness tends to increase from east to west before decreasing sharply on two occasions. Geological analysis reveals that the study area is controlled by regional structures trending north-south (N-S) to northwest (NW) (Figure 13). To the east lies the Quebrada Castro fault system, trending N22°W; this system comprises a series of sub-parallel dextral faults with a minor transpressive component, characterized by the subsidence of the western block (Camus et al., 1991). To the west, there is a system of sub-parallel faults with an average N20°W orientation and no available kinematic data (Vicencio V. et al., 2017). It is also worth noting that between the localities of La Ñipa and Hierro Viejo, the riverbed appears offset (Figure 5)—a key indicator of structural control. The areas crossed by these faults coincide precisely with the locations where fluvio-alluvial deposit thicknesses are lowest; conversely, the greatest thickness occurs to the west of the Quebrada Castro fault system, in the block that—according to Camus (1991)—has subsided.

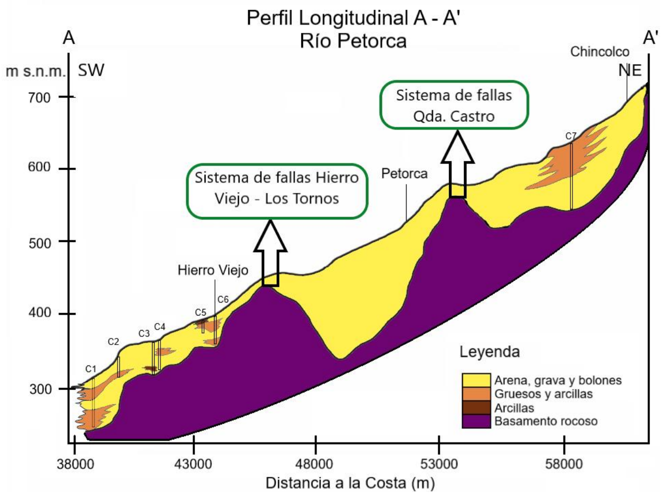

Figure 13. Aquifer profile showing the location of the structures that would control its geometry

These structures could be related to strike-slip fault systems with simple-shear components. This could explain the relief of the bedrock—characterized by drastic changes in slope and depth—as well as the curvature of the river. However, confirming this hypothesis requires a detailed structural survey.

4.4 Water balance 2010–2018

The hydrometeorological balance (Table 1) yields an average annual recharge value of 38.39 hm³/year, while the total input from water supply and sewerage system losses amounts to 0.088 hm³/year.

Table 1. Results obtained from the meteorological balance calculated using the EASY BAL program

Year	Precipitation + Irrigation	ETP Penman	Recharge	Recharge
	(mm/yr)	(mm/yr)	(mm/yr)	hm³/year
2010	540.86	876.44	0.14	0.14
2011	427.64	887.59	33.43	34.05
2012	328.32	924.42	0.00	0.00
2013	278.70	915.70	9.66	9.84
2014	250.17	908.54	24.62	25.08
2015	347.78	918.32	109.75	111.79
2016	479.92	922.25	96.39	98.18
2017	333.44	974.67	65.20	66.41
2018	181.75	970.72	0.00	0.00
Average	352.06	922.07	37.69	38.39

Average withdrawals associated with the granted water rights were estimated at 64.31 hm³/year. Meanwhile, an outflow of 8.83 hm³/year is accounted for at the western boundary of the study area.

Finally, the water balance is calculated assuming a zero river-aquifer relationship, yielding the following calculation:

Inputs - Outputs = Change in storage

38.48 hm^3/a - 73.14 hm^3/a = 34.66 hm^3/a

In previous studies, water balances were calculated from the headwaters to the river mouth; the balance conducted by GCF Ingenieros Ltda. (2013) for the 1950–2010 period shows inflows of 683 L/s (21.46 hm³/year) and outflows of 684 L/s (21.49 hm³/year), whereas the balance for the 2000–2004 period indicates inflows of 571.7 L/s (18.05 hm³/year) and outflows of 570.8 L/s (18.02 hm³/year). Meanwhile, the study most similar to the present research—Álvarez et al. (2015)—conducted a balance for the 1981–2010 period, estimating an inflow of 56.51 hm³/year and an outflow of 70.81 hm³/year.

A comparison of the results from the various water balances reveals a similar pattern, with outflows exceeding inflows. However, in the current instance, the change in storage is significantly greater than in previous cases. This may be because the volume of registered water rights does not necessarily correspond to the amount actually extracted—compounded by the existence of illegal extraction—making it very difficult to calculate the actual extraction figures.

5 Conclusion

- The geometry of the aquifer, like the geology of the area, is primarily controlled by regional fault structures with a preferential North-South to Northwest trend.
- The Petorca aquifer is interpreted as an unconfined aquifer comprising three hydrogeological units associated with fluvio-alluvial deposits, distinguished from one another by their respective clay content.
- The sector's piezometric surface has a gradient of 1% to 2%; groundwater is generally found at a depth of approximately 6 meters in the Hierro Viejo sector, dropping to nearly 30 meters in the Pedegua sector, which indicates a significant and progressive deepening of the piezometric level.
- The aquifer's waters are calcium-bicarbonate type in the Sobrante sector, calcium-bicarbonate-sulfate type in the Pedernal area, and calcium-magnesium-bicarbonate type in the Petorca sector. These varying compositions are linked to the type of recharge received and the dominant activities in each sector.
- Water quality is affected by both natural factors (geology) and anthropogenic factors, such as the rise in nitrate and sulfate levels observed in Petorca Oriente.
- Based on observed hydrochemical variations, if stored water volumes continue to decline, water quality will also deteriorate, potentially rendering the water unfit for human consumption.
- Water availability is impacted by natural factors—such as climate change and the degree of rock fracturing—and anthropogenic factors, including land-use changes and groundwater overexploitation, with the water primarily used for agriculture. If the current extraction regime persists and water-use priorities remain unchanged, habitation in the area is likely to become unsustainable, and the original ecosystem faces total destruction.

Conflicts of interest

The author declares no conflicts of interest regarding the publication of this paper.

References

[1] Álvarez, P., Reyes, H., Cortés, M., & Córdova, A. M. (2015). *Lineamientos estratégicos para la sustentabilidad hídrica de la cuenca de Petorca*. Universidad de La Serena.

[2] Alvarez-Garreton, C. M.-B. (2018). The CAMELS-CL dataset: catchment attributes and meteorology for large sample studies - Chile dataset. *Hydrol. Earth Syst. Sci*., 22, 5817-5846.

[3] ArcGIS Desktop 10.8.1 Educational Academic Departmental Medium Single Use Term License. Tools: ArcGIS Desktop Advanced, ArcGIS 3D Analyst for Pro, ArcGIS Geostatistical Analyst for Pro, ArcGIS Network Analyst for Pro, ArcGIS Publisher for Pro, ArcGIS Spatial Analyst for Pro, ArcGIS Geostatistical Analyst Desktop, ArcGIS Network Analyst for Desktop, ArcGIS Spatial Analyst for Desktop, ArcGIS 3D Analyst for Desktop.

[4] Cade-Idepe Consultores. (2004). *Diagnóstico y clasificación de los cursos y cuerpos de agua según objetivos de calidad*. Vol. 5.Ministerio de Obras Públicas, Dirección General de Aguas, Santiago.

[5] Camus, F., Boric, R., Skewes, M., Castelli, C., Reichhard, E., & Mestre, A. (1991). Geologic, structural, and fluid inclusion studies of El Bronce epithermal vein system, Petorca, central Chile. *Economic Geology*, 86(6), 1317-1345.

[6] Castillo, F. (2008). *Necesidad de agua en las plantaciones de naranjo en Andalucía*. Instituto de Investigación y Formación Agraria y Pesquera, Consejería de Agricultura y Pesca.

[7] Centro de Investigación de Recursos Naturales (CIREN). (2017). *Catastro Frutícola, Región de Valparaíso*.

[8] Cica; Binnie & Partners; Hunting Technical Service Ltda. (1979). *Estudio integral de riego de los valles de Aconcagua, Putaendo, Ligua y Petorca*. Santiago: Comisión de riego.

[9] Custodio, E., & Llamas, M. R. (1996). Hidrología Subterránea, Vol. 1. Barcelona: Omega.

[10] Departamento de Recursos Hídricos; Universidad de Concepción. (2016). *Estudio básico diagnóstico para desarrollar plan de riego en las cuencas de los ríos La Ligua y Petorca*. Concepción.

[11] DGA. (2018). *Seguimiento de la calidad del agua subterránea - Pozos APR región de Valparaíso*. Santiago. ENVI 5.6.1 ENVI Mini Lab Concurrent Process.

[12] Fagundo, J. M. (2010). *Patrones hidrogeoquímicos y origen de la composición química de aguas subterráneas que drenan carbonatos*. Ciudad de la Habana.

[13] FCIHS, C. d. (2009). *Hidrogeología. Conceptos básicos de Hidrología subterránea*. Publicado por Fundación Centro Internacional de Hidrología Subterránea.

[14] GCF Ingenieros Ltda. (2013). *Mejoramiento de agua subterránea para riego Ligua y Petorca*. Santiago.

[15] GCF Ingenieros Ltda. (2011). *Diagnóstico de los recursos subterráneos en el sistema hídrico Ligua y Petorca*. Comisión Nacional de Riego.

[16] Girardi, C., & Recio, J. (2015). *Estudio Hidrogeológico del Baix Ter*. Baix Empordá, Girona. doi: https://doi.org/15004

[17] González-Abraham, Antalia, Fagundo-Castillo, Juan Reynerio, Carrillo-Rivera, José Joel, & Rodríguez- Estrella, Ricardo. (2012). Geoquímica de los sistemas de flujo de agua subterránea en rocas sedimentarias y rocas volcanogénicas de Loreto, BCS, México. *Boletín de la Sociedad Geológica Mexicana*, 64(3), 319-333. Recuperado en 17 de noviembre de 2021, de Recuperado en 17 de noviembre de 2021,
de https://www.scielo.org.mx/scielo.php?script=sci_arttext&pid=S1405-33222012000300005&lng=es&tlng=es .

[18] Instituto Nacional de Estadísticas. (2007). *VII Censo Nacional Agropecuario y Forestal*.

[19] Instituto Nacional de Estadísticas, (2017). *Encuesta de Superficie Sembrada de Cultivos Anuales*.

[20] Lobos G., V. A. (2017). *Manejo hídrico en frutales bajo condiciones edafoclimáticas de Limarí y Choapa*. INIA.

[21] Luebert, F. (2012). Variabilidad climática y bioclimas de la Región de Valparaíso, Chile. *Investigaciones Geográficas*, 41-56.

[22] Ovalle, M. J. (2012). *Estimación de la huella hídrica de cultivos con potencial bioenergético en la provincia de Limarí, región de Coquimbo*, *Chile. Santiago de Chile*.

[23] Pérez, R. (2018). Patrimonio geológico de la comuna de Petorca (32°s - 32°24´s): análisis de lugares de interés geológico y su contextualización en un modelo de evolución paleogeográfico. *Memoria para optar al título de geólogo. Santiago: Universidad de Chile*.

[24] Richard G. Allen, L. S. (1998). *Crop evapotranspiration - Guidelines for computing crop water requirements*. Roma: FAO - Food and Agriculture Organization of the United Nations.

[25] Simler, R. (2018). *Logiciel d'hydrochimie - Water Software Quality Hydrochemistry diagrams. Version 6.59*. France: Laboratoire d'Hydrogéologie d'Avignon.

[26] Superintendencia de Servicios Sanitarios. (2008). *Consumo de agua potable 2007- 2008*.

[27] Vazquez-Suñe, E., & Serrano-Juan, A. (2013). *EASY_BAL v10.7*. Barcelona, España: Universidad Politécnica de Cataluña.

[28] Vélez, M. V. (1999). *Hidráulica de aguas subterráneas*. Medellín, Colombia: Segunda edición, Universidad Nacional de Colombia, Facultad de Minas.

[29] Vicencio V., D. l. (2017). *Informe Geológico de la Comuna de Petorca. Primera etapa de Exploración de la Geodiversidad de la Comuna de Petorca*. Programa de Prácticas Profesionales. Geoparque Valle de Petorca.

Annex

Annex 1. Location and information obtained from different monitoring stations

Station	Measured Parameter	UTM Northing	UTM Easting	First data record	Last data record
Agua Potable Hierro Viejo	Static level	6426647	310475	30-08-1995	23-05-2019
Agua Potable Polcura	Static level	6432125	323775	30-08-1995	01-04-2019
Agua Potable Valle Los Olmos	Static level	6433979	328524	14-12-1995	07-03-2014
Escuela Chalaco	Static level	6437391	329906	15-10-1996	10-09-2009
Los Olmos-Chalaco	Static level	6436276	329181	30-08-1995	01-04-2019
Sociedad Agricola Bellavista	Static level	6429798	319024	30-08-1995	08-10-2018
Rio Pedernal en Tejada	Hydrochemistry - flow	334042	6449855	22-02-1984	23-11-2006
Rio Sobrante en Piñadero	Hydrochemistry - flow	338253	6432848	22-02-1984	22-11-2006
Rio Petorca en Petorca	Hydrochemistry - flow	317861	6430159	03-12-1981	23-11-2006
Chalaco	Precipitation	6438332	331485	01-01-2009	30-11-2018
Sobrante en Hacienda	Precipitation	6432712	330879	01-01-2009	31-12-2018
Trapiche	Precipitation	6432849	336274	01-01-2009	30-11-2018
Hierro Viejo	Precipitation	6426657	313833	01-01-2009	31-12-2018
Pedernal en Hacienda	Precipitation	6447868	330256	01-01-2009	31-12-2018
Petorca en Peñon	Precipitation	6426939	312690	01-01-2009	31-12-2018
Sobrante en Piñadero	Precipitation	6432848	338253	01-12-2012	31-12-2018
Chinolco Iceo Agricola	Temperature	70831666	32222499	01-01-2017	31-12-2018
Salamanca	Temperature	70714	318856	01-01-2017	31-12-2018

Annex 2.. Pearson correlation matrix for the data from the present study

	TDS	T°C	pH	c25°C	cCAL	cC±%	Bal=0	Bal=0	Balan	refaire	Cation	Anion	Ca	Mg	Na	K	Fer	Fe(II)	Fe(III)	Mn	Sr	Li+	Al	NH4	H3O+	HCO3	CO3	Cl	SO4	PO4	NO3	NO2	HS-	S2-	OH-
TDS	1	0.44	0.34	0	1.00	0	0.97	-0.21	0.29	0	1.00	1.00	0.98	0.95	0.92	0.43	0	0	0	0	0	0	0	0	-0.26	0.97	0	0.73	0.90	0	0.04	0	0	0	0.11
T°C	0.44	1	0.19	0	0.43	0	0.47	-0.04	0.11	0	0.43	0.43	0.42	0.41	0.44	0.17	0	0	0	0	0	0	0	0	-0.18	0.47	0	0.26	0.33	0	-0.02	0	0	0	0.03
pH	0.34	0.19	1	0	0.35	0	0.34	-0.03	0.10	0	0.34	0.34	0.36	0.28	0.28	0.19	0	0	0	0	0	0	0	0	-0.68	0.34	0	0.22	0.28	0	0.05	0	0	0	0.70
c25°C	0	0	0	1	0	0	0	0	0	0	0	0	0	0	0	0	0	0	0	0	0	0	0	0	0	0	0	0	0	0	0	0	0	0	0
cCALC	1.00	0.43	0.35	0	1	0	0.95	-0.24	0.32	0	1.00	1.00	0.97	0.96	0.93	0.45	0	0	0	0	0	0	0	0	-0.26	0.96	0	0.75	0.92	0	0.03	0	0	0	0.12
cC±%	0	0	0	0	0	1	0	0	0	0	0	0	0	0	0	0	0	0	0	0	0	0	0	0	0	0	0	0	0	0	0	0	0	0	0
Bal=0% si	0.97	0.47	0.34	0	0.95	0	1	-0.33	0.39	0	0.97	0.96	0.96	0.91	0.88	0.42	0	0	0	0	0	0	0	0	-0.25	0.98	0	0.69	0.78	0	-0.03	0	0	0	0.10
Bal=0% si	-0.21	-0.04	-0.03	0	-0.24	0	-0.33	1	-0.96	0	-0.28	-0.19	-0.27	-0.28	-0.27	-0.36	0	0	0	0	0	0	0	0	-0.01	-0.18	0	-0.31	-0.22	0	0.60	0	0	0	-0.01
Balance	0.29	0.11	0.10	0	0.32	0	0.39	-0.96	1	0	0.36	0.27	0.34	0.36	0.35	0.36	0	0	0	0	0	0	0	0	-0.04	0.25	0	0.35	0.31	0	-0.59	0	0	0	0.05
refaire	0	0	0	0	0	0	0	0	0	1	0	0	0	0	0	0	0	0	0	0	0	0	0	0	0	0	0	0	0	0	0	0	0	0	0
Cations(m	1.00	0.43	0.34	0	1.00	0	0.97	-0.28	0.36	0	2.67	0.99	0.98	0.96	0.93	0.46	0	0	0	0	0	0	0	0	-0.26	0.96	0	0.76	0.91	0	0.00	0	0	0	0.11
Anions(me	1.00	0.43	0.34	0	1.00	0	0.96	-0.19	0.27	0	0.99	2.72	0.97	0.95	0.92	0.42	0	0	0	0	0	0	0	0	-0.26	0.97	0	0.74	0.91	0	0.04	0	0	0	0.11
Ca	0.98	0.42	0.36	0	0.97	0	0.96	-0.27	0.34	0	0.98	0.97	60.9%	0.88	0.84	0.37	0	0	0	0	0	0	0	0	-0.26	0.96	0	0.67	0.87	0	0.00	0	0	0	0.15
Mg	0.95	0.41	0.28	0	0.96	0	0.91	-0.28	0.36	0	0.96	0.95	0.88	21.2%	0.93	0.47	0	0	0	0	0	0	0	0	-0.23	0.89	0	0.78	0.90	0	0.00	0	0	0	0.07
Na	0.92	0.44	0.28	0	0.93	0	0.88	-0.27	0.35	0	0.93	0.92	0.84	0.93	17.1%	0.52	0	0	0	0	0	0	0	0	-0.23	0.88	0	0.79	0.86	0	-0.03	0	0	0	0.04
K	0.43	0.17	0.19	0	0.45	0	0.42	-0.36	0.36	0	0.46	0.42	0.37	0.47	0.52	0.8%	0	0	0	0	0	0	0	0	-0.15	0.37	0	0.63	0.41	0	0.01	0	0	0	0.02
Fer	0	0	0	0	0	0	0	0	0	0	0	0	0	0	0	0	0.0%	0	0	0	0	0	0	0	0	0	0	0	0	0	0	0	0	0	0
Fe(II)	0	0	0	0	0	0	0	0	0	0	0	0	0	0	0	0	0	0.0%	0	0	0	0	0	0	0	0	0	0	0	0	0	0	0	0	0
Fe(III)	0	0	0	0	0	0	0	0	0	0	0	0	0	0	0	0	0	0	0.0%	0	0	0	0	0	0	0	0	0	0	0	0	0	0	0	0
Mn	0	0	0	0	0	0	0	0	0	0	0	0	0	0	0	0	0	0	0	0.0%	0	0	0	0	0	0	0	0	0	0	0	0	0	0	0
Sr	0	0	0	0	0	0	0	0	0	0	0	0	0	0	0	0	0	0	0	0	0.0%	0	0	0	0	0	0	0	0	0	0	0	0	0	0
Li+	0	0	0	0	0	0	0	0	0	0	0	0	0	0	0	0	0	0	0	0	0	0.0%	0	0	0	0	0	0	0	0	0	0	0	0	0
Al	0	0	0	0	0	0	0	0	0	0	0	0	0	0	0	0	0	0	0	0	0	0	0.0%	0	0	0	0	0	0	0	0	0	0	0	0
NH4	0	0	0	0	0	0	0	0	0	0	0	0	0	0	0	0	0	0	0	0	0	0	0	0.0%	0	0	0	0	0	0	0	0	0	0	0
H3O+	-0.26	-0.18	-0.68	0	-0.26	0	-0.25	-0.01	-0.04	0	-0.26	-0.26	-0.26	-0.23	-0.23	-0.15	0	0	0	0	0	0	0	0	0.0%	-0.26	0	-0.16	-0.22	0	-0.08	0	0	0	-0.19
HCO3	0.97	0.47	0.34	0	0.96	0	0.98	-0.18	0.25	0	0.96	0.97	0.96	0.89	0.88	0.37	0	0	0	0	0	0	0	0	-0.26	63.4%	0	0.66	0.78	0	0.04	0	0	0	0.09
CO3	0	0	0	0	0	0	0	0	0	0	0	0	0	0	0	0	0	0	0	0	0	0	0	0	0	0	0.0%	0	0	0	0	0	0	0	0
Cl	0.73	0.26	0.22	0	0.75	0	0.69	-0.31	0.35	0	0.76	0.74	0.67	0.78	0.79	0.63	0	0	0	0	0	0	0	0	-0.16	0.66	0	4.6%	0.71	0	-0.05	0	0	0	0.01
SO4	0.90	0.33	0.28	0	0.92	0	0.78	-0.22	0.31	0	0.91	0.91	0.87	0.90	0.86	0.41	0	0	0	0	0	0	0	0	-0.22	0.78	0	0.71	30.9%	0	-0.05	0	0	0	0.12
PO4	0	0	0	0	0	0	0	0	0	0	0	0	0	0	0	0	0	0	0	0	0	0	0	0	0	0	0	0	0	0.0%	0	0	0	0	0
NO3	0.04	-0.02	0.05	0	0.03	0	-0.03	0.60	-0.59	0	0.00	0.04	0.00	0.00	-0.03	0.01	0	0	0	0	0	0	0	0	-0.08	0.04	0	-0.05	-0.05	0	1.0%	0	0	0	-0.03
NO2	0	0	0	0	0	0	0	0	0	0	0	0	0	0	0	0	0	0	0	0	0	0	0	0	0	0	0	0	0	0	0	0.0%	0	0	0
HS-	0	0	0	0	0	0	0	0	0	0	0	0	0	0	0	0	0	0	0	0	0	0	0	0	0	0	0	0	0	0	0	0	0.0%	0	0
S2-	0	0	0	0	0	0	0	0	0	0	0	0	0	0	0	0	0	0	0	0	0	0	0	0	0	0	0	0	0	0	0	0	0	0.0%	0
OH-	0.11	0.03	0.70	0	0.12	0	0.10	-0.01	0.05	0	0.11	0.11	0.15	0.07	0.04	0.02	0	0	0	0	0	0	0	0	-0.19	0.09	0	0.01	0.12	0	-0.03	0	0	0	0.1%

About the author

Justinne Rybertt Goldammer is a geologist from Andrés Bello University. Her undergraduate studies focused on hydrogeology, specifically within the Petorca River basin. She has academic experience in fields such as hydrogeology and structural geology. She currently works as a professional at the Climate Action Center of the Pontifical Catholic University of Valparaíso, contributing to the development of climate change adaptation plans; additionally, she is a member of the Hydro-social Territories and Climate Change Laboratory at the same university and the Isotopic Analysis Laboratory at Andrés Bello University.